IEEE Access
Multidisciplinary | Rapid Review | Open Access Journal

Received November 26, 2018, accepted December 13, 2018, date of publication December 24, 2018,
date of current version January 23, 2019.

*Digital Object Identifier 10.1109/ACCESS.2018.2889620*

# Interference Mitigation for 5G Millimeter-Wave Communications

**DIMITRIOS SIAFARIKAS, (Graduate Student Member, IEEE),**
**ELIAS A. ALWAN, (Member, IEEE),**
**AND JOHN L. VOLAKIS, (Fellow, IEEE)**
Department of Electrical and Computer Engineering, Florida International University, Miami, FL 33174, USA

Corresponding author: Dimitrios Siafarikas (siafarikas@fiu.edu)

This research was supported in part by the NSF grant award 1547221 and ONR grant award N00014-16-1-2253.

**ABSTRACT** We present a novel ultra-wideband low-cost transmit/receive architecture with reduced power and hardware requirements, which includes interference mitigation capabilities and accommodates multiple users. Specifically, a novel encoding approach is introduced to multiplex signals across large bandwidths and achieve secure communication and interference mitigation through spread signals. In this paper, a detailed description of the proposed high data rate system architecture is presented. Simulations are also provided in the presence of high-power interferers with eight concurrent users. To assess the performance and impact of the encoding/decoding process, a noise analysis was conducted for the transmitter and receiver chains. Specifically, bit error rate curves are generated at different stages of the system. The measurements show interference margin ratios improvement by at least 16 dB.

**INDEX TERMS** 5G communication, millimeter wave, CDMA, beamforming, interference, co-existence.

## I. INTRODUCTION

There are several methods in the literature to mitigate signal interference in radio frequency (RF) communications. In addition to filtering, other methods may employ active interference cancellation to suppress interference at the receiver front-end [1]–[5]. Among available methods, interference cancellation techniques can be classified into several approaches [6]: space, time, frequency, time-frequency, and code domains. Space domain methods use antenna arrays with adaptive beamforming [7] to suppress interfering signals by steering the beam to different directions or by placing nulls along the direction of the interfering signals [8]–[11]. In time-domain methods, adaptive filtering is performed using finite impulse response (FIR) and infinite impulse response (IIR) filters [12]–[14]. However, these interference cancellation methods are limited to narrowband interferers and incur hardware complexity. Also, frequency domain methods have been proposed for interference rejection [15]–[18]. A major drawback for the latter is hardware complexity due to requiring Fast Fourier transform (FFT), inverse FFT, or wavelet transform blocks as part of the hardware. Additionally, windowing blocks are needed to avoid significant spectral leakage [14], implying higher costs. Further, time-frequency excision techniques require an estimate of the interferer instantaneous frequency [19], implying even more complex hardware. A sophisticated orthogonal-like Gabor expansion may also be required to estimate the interferer signal prior to subtracting it from the input [20].

Most of the above interference suppression techniques are limited in terms of their spectral and spatial filtering, and suffer from limitations in hardware and digital cancellation techniques [1]–[4]. That is, in presence of high interference levels, these techniques, if implemented individually, fall short to achieving enough suppression. Also, most require previous knowledge of the interferer's position, channel, and signal identity [3]. Of course, in realistic scenarios, and when communicating across wide bandwidths, interferers are unknown to the receiver. Therefore, more advanced techniques are required to suppress interference and avoid signal fratricide.

Alternatively, interference rejection can also be achieved by employing direct sequence spread spectrum modulation (DSSS) [21]. Popular communication systems typically use code domain for interference cancellation. For instance, Wi-Fi, CDMA2000, and Global Positioning System (GPS) use Barker codes [22], a combination of Walsh and Gold codes [23], and long Gold codes [24], respectively. The key advantage of spread spectrum modulation is immunity to noise and multipath distortion, including interference mitigation. Also, Code Division Multiplexing (CDM) is known for its high spectral efficiency as compared to other

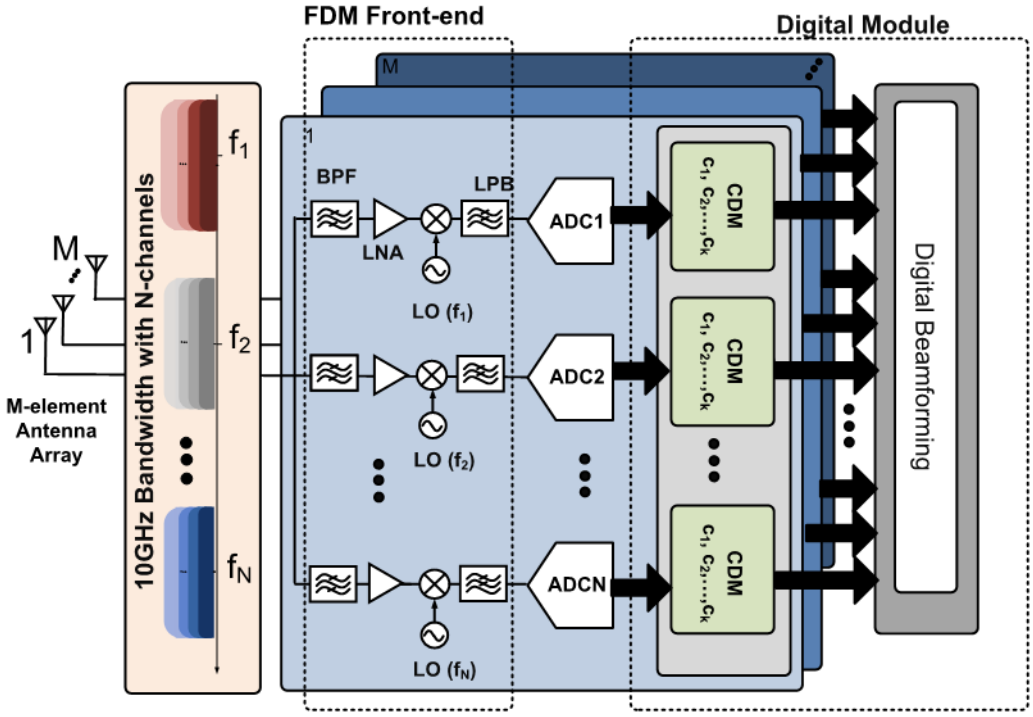


**FIGURE 1.** Hybrid F/CDM receiver architecture for ultra-wideband multi-user communications. The RF front-end consists of a frequency division demultiplexing block to channelize the multi-GHz signal. Each sub-channel can accommodate up to K-users, each uniquely encoded with a CDM code.

double-sided modulation schemes [25]. CDM is also known to be robust against narrowband interference. Further, the random properties of CDM code sequences make them attractive when deployed in fading channel environments [25]. This is because it can discard the samples generated by multipath propagation [25]. In addition, protection against channel perturbation can be achieved when implementing CDM with channel coding, which provides error detection and correction features. That is, coding gain increases the interferer's power margin and receiver's resilience against high power malicious attacks [26]–[29].

With this in mind, in this paper, we present for the first time, an ultra-wideband (UWB) receiver architecture with interference mitigation that exploits the spatial and spectral diversity for high speed multi-user communication.

Some of the unique features of our system include: 1) up to 27 dB of combined gain, 2) enhanced security at the physical layer, 3) large instantaneous bandwidth access of 1.3 GHz allowing for wider signal spreading to enable strong interference mitigation, and 3) 10-fold increase in data rates as compared to other CDMA protocols.

The block diagram of this architecture is shown in Fig. 1 and is based on a hybrid Frequency/Coding Division Multiplexing (F/CDM) front-end operating across a few gigahertz (e.g. 10 GHz) of instantaneous bandwidth. The goal is to deliver high data rates to multiple users (see Fig. 2). Using FDM, it is possible for signals with large instantaneous bandwidth to be received and channelized at the RF front-end into smaller sub-channels to accommodate bandwidth constraints imposed by RF components such as low noise amplifiers (LNA), filters, mixers, analog-to-digital (ADC) and digital-to-analog (DAC) converters and digital modules (field-programmable gate arrays (FPGAs), application-specific integrated circuits (ASICs)). Also, with smaller sub-channels (*viz.* <1.5 GHz), a more reasonable transmission can be achieved taking into account bandwidth limitations posed by the power amplifiers (PAs). Further, use of CDM implies large number of users per sub-channel and significant immunization against high power malicious interferers. In addition to F/CDM, to relax hardware requirements, our hybrid receiver employs on-site coding (OSC) at the analog baseband. As such, it can combine all signal paths pertaining to each sub-channel and digitize them using a single ADC. OSC has been previously implemented and verified in [30]–[35] for digital beamforming applications, and has demonstrated significant hardware, power, and cost reduction while maintaining its performance intact. For the sake of simplicity, the OSC stage was omitted from the block diagram.

In this paper, an analysis of the wideband multi-user architecture is presented. Specifically, in the first part of the paper, the maximum number of users is optimized. To do so, the available 10 GHz bandwidth is sub-divided into 7 sub-channels, 1.4 GHz each. For each sub-channel, the maximum number of users that can be accommodated without compromising performance is examined. To do so,

Bit-error-rate (BER) is calculated to determine the maximum number of allowable users per sub-channel. Subsequently, we evaluate system performance in presence of high power interferers. The goal is to evaluate the maximum interferer-to-signal ratio (ISR) for uninterrupted communication for all users. Results show that very little degradation occurs for up to 8 users using the same band, in presence of an interferer at 10 dB above the received signal.

This paper is organized as follows. Section II provides a detailed description of the proposed architecture and its advantages. In Section III, two case studies are used to assess the performance of this novel hybrid system. Section IV describes the measurements and presents measured results and simulations.

## II. DESCRIPTION OF THE HYBRID F/CDM RECEIVER ARCHITECTURE

The hybrid F/CDM receiver employs an UWB antenna array with continuous operation across very large bandwidths (*viz.* 10 GHz). These arrays are based on tightly coupled dipole elements with compact feeding networks. They have already been designed and implemented to deliver more than 13.5:1 continuous impedance bandwidth [36], [37]. Such a large bandwidth enables high data rate communications and allows for UWB beamforming. The benefits of such arrays can only be realized when paired with suitable back-end architecture. However, as already mentioned, RF electronics are mostly narrowband. In this paper, we present a novel receiver architecture that can accommodate wideband signals using multi-GHz of instantaneous bandwidth. Central to its performance is a frequency division multiplexing front-end. As shown in Fig. 2, the large bandwidth is divided into $N-$sub-channels. Each sub-channel covers a much smaller bandwidth and has its own dedicated RF electronics. Also, to allow for multi-user communication and hence maximize usage of communications resource (CR), we assume that multiple users are communicating with the receiver at the same time using the same sub-channel. This is possible using code division multiplexing (CDM). To do so, we assume that each user's signal is encoded with a unique Gold code, up-converted to a specific frequency band. This is illustrated in Fig. 3.

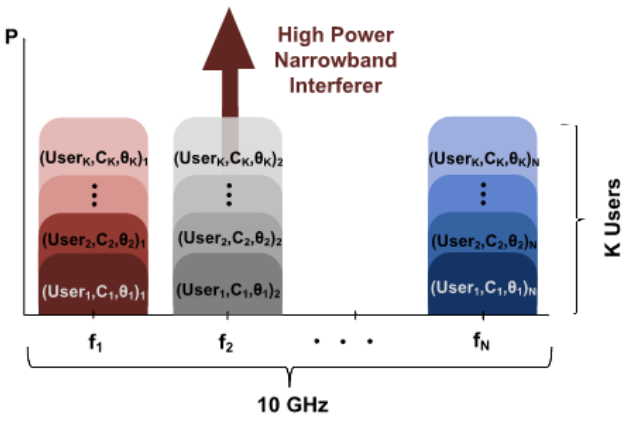


**FIGURE 2.** Frequency domain representation of an N-channel signal across 10 GHz, with each channel accommodating up to K-users. Such composite signal can be demultiplexed and decorrelated using the hybrid F/CDM front-end. Also shown a high power interferer in the second band.

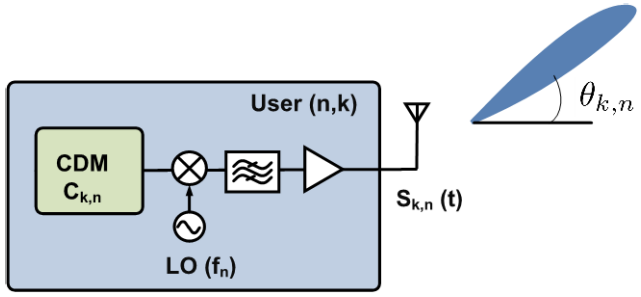


**FIGURE 3.** User $(k, n)$ simplified transmitter architecture. The transmitted signal is coded with a Gold code $c_{k,n}$ and upconverted to the $n^{th}$ frequency band.

All users (total of $K$-users) transmitting over the same sub-channel are encoded with the same family of Gold codes, $c_{k,n}$, for each of the $k^{th}$ user, where $k$ corresponds to the number of users and $n$ to the frequency band. We note that the spatial distribution of these user is random. That is, each user is transmitting at an angle $\theta_{k,n}$.

The total composite signal at the receiver is the sum of all coded signals across all $N$-frequency bands. In other words,

$$r(t) = \sum_{n=1}^{N} \sum_{k=1}^{K} s_{k,n}(t) + n_{k,n}(t) \tag{1}$$

In the above, $s_{k,n}(t)$ and $n_{k,n}(t)$ refers to the coded signal and the channel noise of the $k^{th}$ user, respectively. As an example, we assume that a 10 GHz instantaneous bandwidth is available to deliver high data rates to multiple users. Each user's signal is also assumed to have a bit-rate $R_b = 10$ Mbps rate and is spread with Gold code sequence of length 127 across 1.27 GHz [38]. As a result, a process gain can be achieved, equal to

$$\begin{aligned} G_p &= 10log_{10}\left(\frac{Spread\ Bandwidth}{Bit\ Rate}\right) \\ &= 21.03\ dB \end{aligned} \tag{2}$$

After spreading, each user signal is up-converted to a different channel, depending on the interference level. In this case, we will have up to 7 different channels, each 1.27 GHz wide and to accommodate a large number of users (see Fig. 2). We note that in addition to processing gain, coding gain can be achieved using conventional channel codes. As such, a 6 dB channel coding gain using Turbo codes can be also achieved [39], raising the total combined gain to ≈27 dB.

## III. SYSTEM PERFORMANCE IN PRESENCE OF INTERFERENCE

### A. ERROR PROBABILITY

An advantage of using large bandwidth is interference mitigation. Below, we evaluate the maximum number of users that

can be accommodated by the same channel in presence of high-power interference. Throughout the study, we assume a Binary Phase Shift Keying (BPSK) modulation for simplicity. Our initial analysis (see Fig. 4) shows that BER degradation is small when combining up to 8 users in a channel. On average, 2 dB of degradation is observed. We note that the blue curve in Fig. 4 refers to the worst case error and is calculated using [40]

$$P_{BPSK} \leq Q\left(\left[1 - \frac{2C_c(N_c - 1)}{L_c}\right]\sqrt{2E_b/N_0}\right) \quad (3)$$

where $Q$ is the Q-function which represents the tail distribution function of the standard normal distribution [41], $E_b$ denotes the average bit energy, $C_c$ is the cross-correlation of the Gold codes, $N_c$ refers to the number of users, and $L_c$ is the length of the Gold Code. Referring to Fig. 4, it is clear that the computed average BER for 8 users falls between the theoretical lower limit and worst-case BER curve [40].

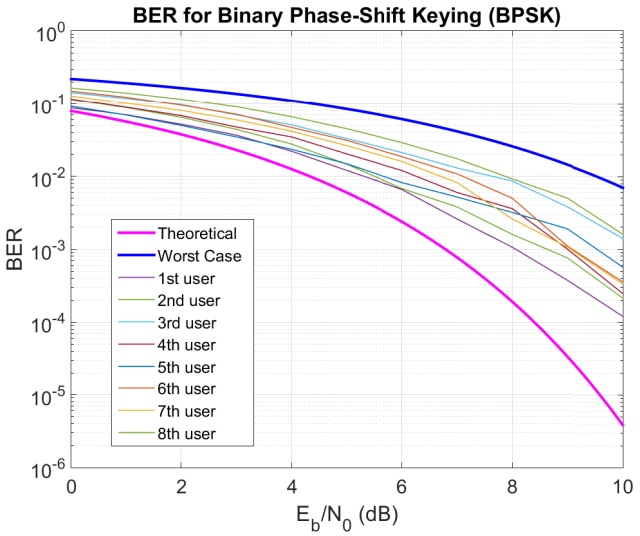


**FIGURE 4.** BER curves for 8 users communicating using the same frequency band.

Next, we conducted simulations in presence of a narrowband interferer. Both coded and uncoded signals were considered. For uncoded signals, we injected an interferer in the communication link of a single user, without any interference mitigation technique. More specifically, interference was introduced as a single, high power tone within the transmission bandwidth. This was done using a time-domain waveform added to the transmitted signal after passing it through the AWGN channel. As shown in Fig. 5, the probability of error increases significantly as the Interference-to-Signal Ratio (ISR) increases. Notably, for ISR = 20 dB, the signal is no longer recoverable.

However, when F/CDM is employed, as in Fig. 6, interference 10 dB above the signal only causes 1 of degradation with 2 concurrent users. Further, with 8 concurrent users, only 3 db of degradation is observed. That is, the proposed Gold codes with spreading provide strong interference mitigation.

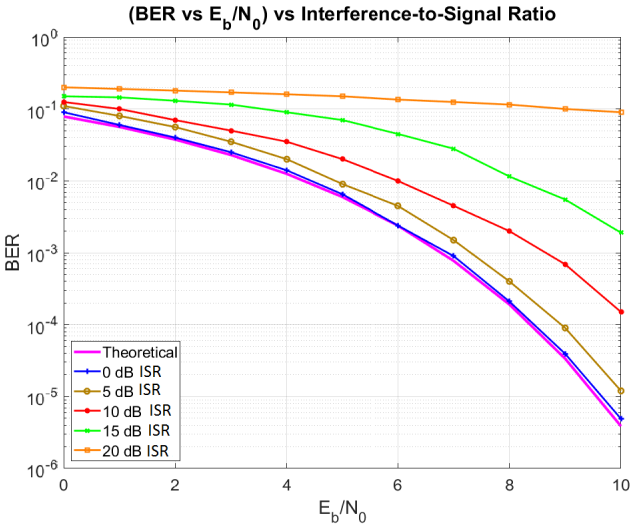


**FIGURE 5.** BER curves for 1 user communicating in presence of interference.

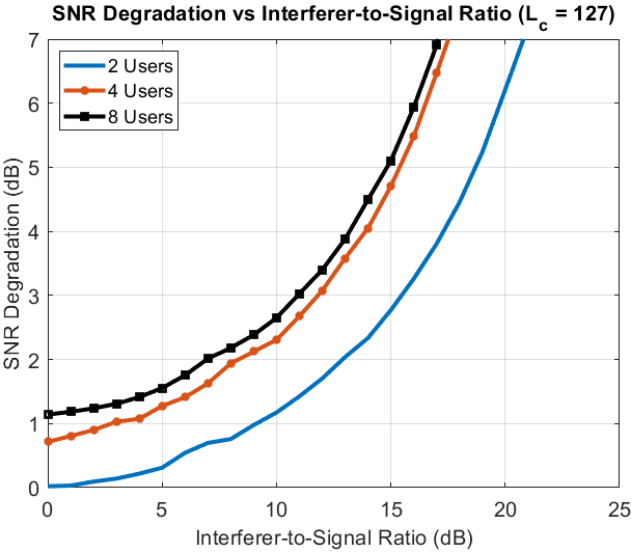


**FIGURE 6.** SNR degradation vs Interference-to-Signal ratio for 2, 4, and 8 concurrent users.

Notably, degradation for 8 users is only 0.8 dB more than degradation for 4 users. This is due to the nature of the spread signal. In other words, the resulting spread signal does not have a flat frequency response and is affected differently depending on the interferer's frequency of operation.

### *B. CHANNEL CODING GAIN FROM TURBO CODES*

As noted earlier, the CDM operation provided 21 dB of processing gain. An additional 6 dB of gain can be achieved using Turbo codes [39], implying a total combined gain of 27 dB. As it is well known, Turbo codes refer to a class of convolutional codes whose BER performance approach the Shannon limit of −1.59 dB. Specifically, we employed CDM and rate 1/2 Turbo codes. For this coding scheme, the average BER

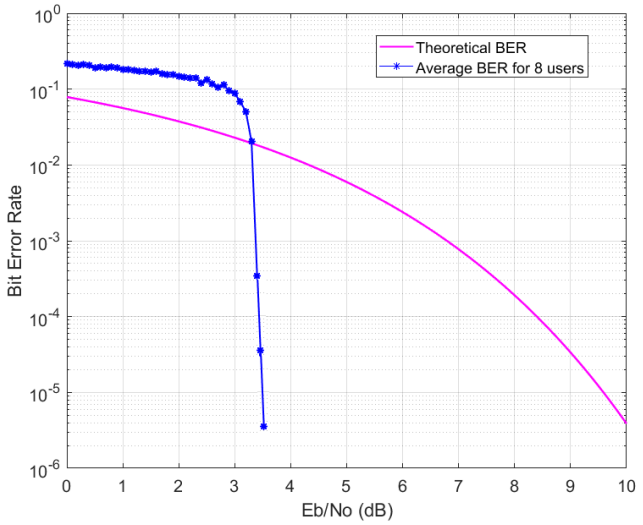


**FIGURE 7.** BER performance for each of the 8 users. Each user employs CDM and Turbo Codes.

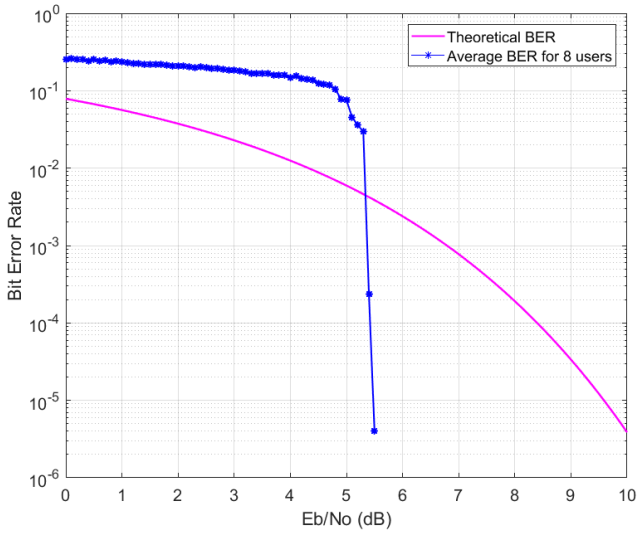


**FIGURE 8.** BER performance for each of the 8 users in presence of a single high-power interferer. Each user employs CDM and Turbo Codes.

performance is shown in Fig. 7. It is observed that all users experience significant coding gain as a result of combining CDM and Channel coding (as compared to a single-user uncoded BPSK communication link).

As a final simulation, Code Division Multiplexing and Channel Coding were tested in presence of a single high-power interferer. The BER for 8 users are shown in Fig. 8. We again observe that the total average degradation is only 3 dB as compared to curves shown in Fig. 7. That is, interference does not affect BER significantly.

## IV. MEASUREMENTS

### A. MEASUREMENT SETUP

In this section, we carry out measurements to verify the achieved processing gain via the proposed UWB

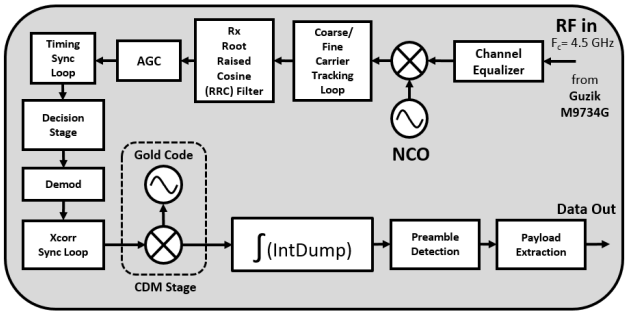


**FIGURE 9.** Practical UWB receiver implemented in software defined fashion.

multi-user hybrid F/CDM transceiver architecture. To do so, we employed an equipment setup using Keysight (M8190A [42] as a transmitter. The latter allows up to 6 GHz bandwidth and employs Guzik Technologies equipment (M9734G [43]) as a receiver, allowing operation across 6.5 GHz. Both the transmitter and receiver were designed in a software defined fashion to minimize cost. Further, Direct RF sampling was used to remove the bottleneck of complex RF front-ends for ultra-wideband signals. For this experiment, we focused on the interference suppression capabilities of the link. Therefore, we used a single antenna at the transmitter and receiver.

The transceiver operation is as follows: After creating the signal in baseband, the Keysight M8190 Arbitrary Waveform Generator was used to Digitally Up-Convert (DUC) and transmit the signal at 4.5 GHz center frequency. A standard horn antenna was then used to transmit the signal. The receiver architecture was implemented using the M9734G digitizer as shown in Fig. 9. Notably, this digitizer employs interleaved ADCs to achieve 20 GSPS sampling rates. A photo of the actual hardware setup is shown in Fig. 10. As already mentioned, the channel bandwidth is approximately 1.3 GHz and, as noted, multiple users can readily occupy the same bandwidth without appreciable BER degradation.

Below we proceed to carry out BER measurements to assess improvements in processing gain using CDM spreading across 1.3 GHz bandwidth. First, we carry out measurements without interference and then proceed to do the same in presence of an interferer. Channel coding was not implemented in this measurement study.

### B. SYSTEM CHARACTERIZATION

The first step towards link characterization is the estimation of losses. To do so, the theoretical and measured BERs were measured for a single BPSK communication link. An initial set of measurements were done using BPSK modulation as shown in Fig. 11. It was found that for a BER $= 10^{-3}$, an approximate loss of 3 *dB* was observed due to imperfections such as cable losses, mismatches and, possibly, due to a non-optimized implementation of the system (timing loops,

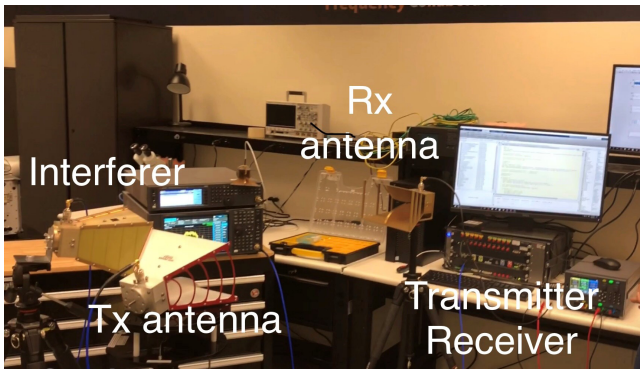


**FIGURE 10.** Measurements hardware setup.

symbol tracking loops, etc). Therefore, we will assume that $L_{sys} \approx 3\ dB$.

In a second set of measurement, we injected an interferer to the link. Specifically, the intereferer's power was varied by 14 $dB$ by adjusting its power at $f = 4.5$ GHz, viz. in the middle of the operational bandwidth. It was found that for a signal-to-interference-plus-noise level of 18 $dB$, we can achieve $10^{-3}$ BER as shown in Fig. 11. This is 8 $dB$ degradation in our interference margin as compared to the measured BPSK link with no interference.

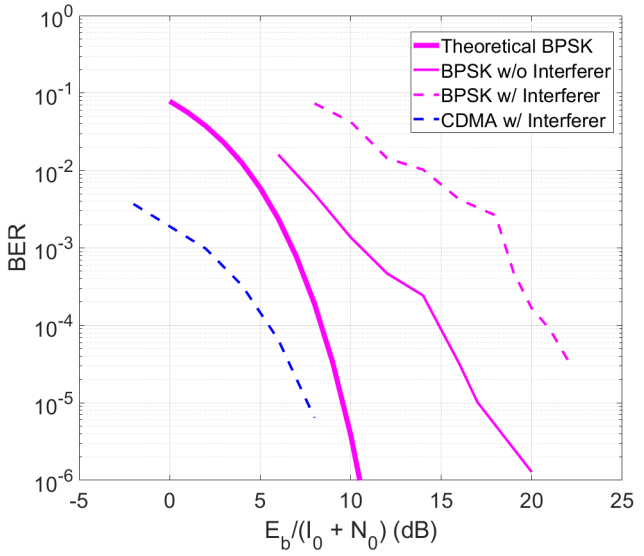


**FIGURE 11.** Theoretical and measured BER for a BPSK communication link and CDMA link in absence and presence of a single high-power interferer.

In another measurement, we introduce CDM in the communication link. Fig. 11 shows the measured BER data in presence of an interfering signal. These measurements were obtained by running the transmit/receive system for several hours using a randomized set of codes and recording the BER across various SNR values. As seen, CDM with spreading length $L_c = 127$ across a 1.3 GHz, implies significant reduction in BER. Specifically, we found that for BER $= 10^{-3}$, we only need $E_b/I_0 = 2\ dB$ implying a gain of 8 $dB$ gain. In total, we achieved 16 $dB$ of gain margin. This corresponds to the processing gain. Theoretically, our processing gain should be 21 $dB$. That is, 5 $dB$ loss is due to $L_{sys}$ and other losses due to interference injection.

## V. CONCLUSIONS

We presented a novel receiver architecture for wideband multi-user communication links with interference mitigation. The receiver includes several innovations:

1) Multi-user connectivity using hybrid Frequency and Coding Division Multiplexing (F/CDMA).
2) CDM signal spreading with up to 40 dB of processing gain if channel coding is employed.
3) Interference mitigation due to UWB code spreading.
4) Ten-fold increase in peak data rates as compared to other CDMA protocols [44], [45].

Overall, it was demonstrated that the available large bandwidth with code spreading can lead to substantial processing gain, even in presence of interference. These capabilities were demonstrated, for the first time, experimentally.

## REFERENCES

[1] T. D. Werth, C. Schmits, R. Wunderlich, and S. Heinen, "An active feedback interference cancellation technique for blocker filtering in RF receiver front-ends," *IEEE J. Solid-State Circuits*, vol. 45, no. 5, pp. 989–997, May 2010.

[2] A. Raghavan, E. Gebara, E. M. Tentzeris, and J. Laskar, "Analysis and design of an interference canceller for collocated radios," *IEEE Trans. Microw. Theory Techn.*, vol. 53, no. 11, pp. 3498–3508, Nov. 2005.

[3] G. Karawas, K. Goverdhanam, and J. Koh, "Wideband active interference cancellation techniques for military applications," in *Proc. 5th Eur. Conf. Antennas Propag. (EUCAP)*, Apr. 2011, pp. 390–392.

[4] J. T. Chiang and Y.-C. Hu, "Dynamic jamming mitigation for wireless broadcast networks," in *Proc. 27th Conf. Comput. Commun.*, Apr. 2008, pp. 1211–1219.

[5] H. Yamaguchi, "Active interference cancellation technique for MB-OFDM cognitive radio," in *Proc. 34th Eur. Microw. Conf.*, vol. 2, Oct. 2004, pp. 1105–1108.

[6] Y.-R. Chien, "Design of GPS anti-jamming systems using adaptive notch filters," *IEEE Syst. J.*, vol. 9, no. 2, pp. 451–460, Jun. 2015.

[7] M. Jones, "The civilian battlefield: Protecting GNSS receivers from interference and jamming," *Inside GNSS*, vol. 6, no. 2, pp. 40–49, Mar./Apr. 2011.

[8] Y. D. Zhang and M. G. Amin, "Anti-jamming GPS receiver with reduced phase distortions," *IEEE Signal Process. Lett.*, vol. 19, no. 10, pp. 635–638, Oct. 2012.

[9] I. J. Gupta *et al.*, "Non-planar adaptive antenna arrays for GPS receivers," *IEEE Antennas Propag. Mag.*, vol. 52, no. 5, pp. 35–51, Oct. 2010.

[10] D. Lu, R. Wu, and H. Liu, "Global positioning system anti-jamming algorithm based on period repetitive CLEAN," *IET Radar, Sonar Navigat.*, vol. 7, no. 2, pp. 164–169, Feb. 2013.

[11] R. Iltis and L. Milstein, "An approximate statistical analysis of the Widrow LMS algorithm with application to narrow-band interference rejection," *IEEE Trans. Commun.*, vol. COMM-33, no. 2, pp. 121–130, Feb. 1985.

[12] D. Borio, L. Camoriano, and L. L. Presti, "Two-pole and multi-pole notch filters: A computationally effective solution for GNSS interference detection and mitigation," *IEEE Syst. J.*, vol. 2, no. 1, pp. 38–47, Mar. 2008.

[13] L. A. Rusch and H. V. Poor, "Narrowband interference suppression in CDMA spread spectrum communications," *IEEE Trans. Commun.*, vol. 42, no. 234, pp. 1969–1979, Feb. 1994.

[14] P. T. Capozza, B. J. Holland, T. M. Hopkinson, and R. L. Landrau, "A single-chip narrow-band frequency-domain excisor for a global positioning system (GPS) receiver," *IEEE J. Solid-State Circuits*, vol. 35, no. 3, pp. 401–411, Mar. 2000.

[15] Z. Wang, M. Lv, and B. Tang, "Paper application of partial coefficient update LMS algorithm to suppress narrowband interference in DSSS system," in *Proc. Int. Conf. Commun. Softw. Netw.*, Feb. 2009, pp. 275–278.
[16] L. Zhang, S. Yuan, Y. Chen, and J. Yang, "Narrowband interference suppression in DSSS system based on frequency shift wavelet packet transform," in *Proc. 9th Int. Conf. Electron. Meas. Instrum.*, Aug. 2009, pp. 2-333–2-337.
[17] Y.-R. Chien, "Hybrid successive continuous wave interference cancellation scheme for global positioning system receivers," *J. Eng.*, vol. 2013, no. 7, pp. 7–14, Jul. 2013. [Online]. Available: https://ieeexplore.ieee.org/document/8410957
[18] Y.-R. Chien, Y.-C. Huang, D.-N. Yang, and H.-W. Tsao, "A novel continuous wave interference detectable adaptive notch filter for GPS receivers," in *Proc. IEEE Global Telecommun. Conf. (GLOBECOM)*, Dec. 2010, pp. 1–6.
[19] L. Cohen, *Time-Frequency Analysis*. Upper Saddle River, NJ, USA: Prentice-Hall, 1995, vol. 778.
[20] S. Savasta, L. L. Presti, and M. Rao, "Interference mitigation in GNSS receivers by a time-frequency approach," *IEEE Trans. Aerosp. Electron. Syst.*, vol. 49, no. 1, pp. 415–438, Jan. 2013.
[21] M. B. Pursley and T. C. Royster, "Coding alternatives for high-rate direct-sequence spread spectrum," in *Proc. Mil. Commun. Conf.*, vol. 2, Oct./Nov. 2004, pp. 892–898.
[22] S. Ahmed, M. Khurram, and M. A. Khan, "Matlab based implementation of IEEE 802.11b DSSS transmitter," in *Proc. 13th Int. Bhurban Conf. Appl. Sci. Technol. (IBCAST)*, Jan. 2016, pp. 624–630.
[23] S. Willenegger, "CDMA2000 physical layer: An overview," *J. Commun. Netw.*, vol. 2, no. 1, pp. 5–17, Mar. 2000.
[24] M. M. Hafidhi, E. Boutillon, and C. Winstead, "Reliable gold code generators for GPS receivers," in *Proc. IEEE 58th Int. Midwest Symp. Circuits Syst. (MWSCAS)*, Aug. 2015, pp. 1–4.
[25] L. Hanzo, L.-L. Yang, E.-L. Kuan, and K. Yen, *Single- and Multi-Carrier DS-CDMA: Multi-User Detection, Space-Time Spreading, Synchronisation, Networking and Standards*. Hoboken, NJ, USA: Wiley, 2003.
[26] D. J. Costello, Jr., and G. D. Forney, "Channel coding: The road to channel capacity," *Proc. IEEE*, vol. 95, no. 6, pp. 1150–1177, Jun. 2007.
[27] V. Pless, "Decoding the Golay codes," *IEEE Trans. Inf. Theory*, vol. IT-32, no. 4, pp. 561–567, Jul. 1986.
[28] A. Gabay, M. Kieffer, and P. Duhamel, "Joint source-channel coding using real BCH codes for robust image transmission," *IEEE Trans. Image Process.*, vol. 16, no. 6, pp. 1568–1583, Jun. 2007.
[29] V. Tarokh, H. Jafarkhani, and A. R. Calderbank, "Space-time block codes from orthogonal designs," *IEEE Trans. Inf. Theory*, vol. 45, no. 5, pp. 1456–1467, Jul. 1999.
[30] E. A. Alwan, S. B. Venkatakrishnan, A. A. Akhiyat, W. Khalil, and J. L. Volakis, "Code optimization for a code-modulated RF front end," *IEEE Access*, vol. 3, pp. 260–273, 2015.
[31] S. B. Venkatakrishnan, A. A. Akhiyat, E. A. Alwan, and J. L. Volakis, "Dual-band validation of on-site coding receiver using ultra-wideband antenna array at C, X and Ku-bands," in *Proc. IEEE Int. Symp. Antennas Propag. (APSURSI)*, Jun./Jul. 2016, pp. 1655–1656.
[32] E. A. Alwan, A. A. Akhiyat, W. Khalil, and J. L. Volakis, "Analytical and experimental evaluation of a novel wideband digital beamformer with on-site coding," *J. Electromagn. Waves Appl.*, vol. 28, no. 12, pp. 1401–1429, Aug. 2014.
[33] S. B. Venkatakrishnan, A. Akhiyat, E. A. Alwan, W. Khalil, and J. L. Volakis, "Realization of a novel on-site coding digital beamformer using FPGAs," in *Proc. USNC-URSI Radio Sci. Meeting (Joint AP-S Symp.)*, Memphis, TN, USA, Jul. 2014, p. 196.
[34] E. A. Alwan, A. Akhiyat, M. LaRue, W. Khalil, and J. L. Volakis, "Low cost, power efficient, on-site coding receiver (OSCR) for ultra-wideband digital beamforming," in *Proc. IEEE Int. Symp. Phased Array Syst. Technol.*, Boston, MA, USA, Oct. 2013, pp. 202–206.
[35] S. B. Venkatakrishnan, D. K. Papantonis, A. A. Akhiyat, E. A. Alwan, and J. L. Volakis, "Experimental validation of on-site coding digital beamformer with ultra-wideband antenna arrays," *IEEE Trans. Microw. Theory Techn.*, vol. 65, no. 11, pp. 4408–4417, Nov. 2017.
[36] M. H. Novak and J. L. Volakis, "Ultrawideband antennas for multiband satellite communications at UHF–Ku frequencies," *IEEE Trans. Antennas Propag.*, vol. 63, no. 4, pp. 1334–1341, Apr. 2015.
[37] W. F. Moulder, K. Sertel, and J. L. Volakis, "Superstrate-enhanced ultrawideband tightly coupled array with resistive FSS," *IEEE Trans. Antennas Propag.*, vol. 60, no. 9, pp. 4166–4172, Sep. 2012.
[38] F. Adachi, D. Garg, S. Takaoka, and K. Takeda, "Broadband CDMA techniques," *IEEE Wireless Commun.*, vol. 12, no. 2, pp. 8–18, Apr. 2005.
[39] C. Berrou, A. Glavieux, and P. Thitimajshima, "Near shannon limit error-correcting coding and decoding: Turbo-codes. 1," in *Proc. IEEE Int. Conf. Commun.*, vol. 2, May 1993, pp. 1064–1070.
[40] M. Pursley, "Performance evaluation for phase-coded spread-spectrum multiple-access communication—Part I: System analysis," *IEEE Trans. Commun.*, vol. COMM-25, no. 8, pp. 795–799, Aug. 1977.
[41] J. G. Proakis, M. Salehi, N. Zhou, and X. Li, *Communication Systems Engineering*, vol. 2. Upper Saddle River, NJ, USA: Prentice-Hall, 1994.
[42] *M8190A 12 GSa/s Arbitrary Waveform Generator*. Accessed: Jun. 25, 2018. [Online]. Available: https://www.keysight.com/en/pd-1969138-pn-M8190A/12-gsa-s-arbitrary-waveform-generator?cc=US&lc=eng
[43] *Guzik Technical Enterprises. ADC6000 Series 8-bit Digitizers—Guzik Technical Enterprises*. Accessed: Jun. 25, 2018. [Online]. Available: http://www.guzik.com/product/adc6000-series-8-bit-digitizers/
[44] R. Prasad and T. Ojanpera, "An overview of CDMA evolution toward wideband CDMA," *IEEE Commun. Surveys*, vol. 1, no. 1, pp. 2–29, 1st Quart., 1998.
[45] Y.-K. Kim and B. K. Yi, "3G wireless and CDMA2000 1× evolution in Korea," *IEEE Commun. Mag.*, vol. 43, no. 4, pp. 36–40, Apr. 2005.

**DIMITRIOS SIAFARIKAS** (GS'15) was born in Larisa, Greece, in 1991. He received the Diploma degree in electrical and computer engineering from the Democritus University of Thrace, Xanthi, Greece, in 2015, and the M.Sc. degree from The Ohio State University, in 2017.

He is currently pursuing the Ph.D. degree with the RFCOM Lab, Florida International University, Miami, FL, USA. His current research interests include software-defined radios, RF systems for ultra-wideband communications, millimeter-wave systems for 5G, and interference suppression via spread spectrum techniques.

**ELIAS A. ALWAN** (GS'07–M'10) was born in Aitou, Lebanon, in 1984. He received the B.E. degree *(summa cum laude)* in computer and communication engineering from Notre Dame University–Louaize, Zouk Mosbeh, Lebanon, in 2007, the M.E. degree in electrical engineering from the American University of Beirut, Beirut, Lebanon, in 2009, and the Ph.D. degree in electrical and computer engineering from The Ohio State University (OSU), Columbus, OH, USA, in 2014. He was a Senior Research Associate with the ElectroScience Laboratory, OSU, from 2015 to 2017. He is currently an Assistant Professor with the ECE Department, Florida International University. His research interests include the areas of antennas and radio frequency systems with particular focus on ultra-wideband (UWB) communication systems, including UWB arrays, reduced hardware and power efficient communication back-ends, and millimeter-wave technologies for 5G applications. He has been a Phi Kappa Phi Member, since 2010.

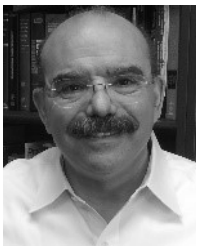

**JOHN L. VOLAKIS** (S'77–M'82–SM'89–F'96) was born in Chios, Greece, in1956, and immigrated to the USA, in 1973. He received the B.E. degree *(summa cum laude)* from Youngstown State University, Youngstown, OH, USA, in 1978, and the M.Sc. and Ph.D. degrees from The Ohio State University, Columbus, OH, USA, in 1979 and 1982, respectively.

He started his career with Rockwell International (1982–1984), now Boeing. In 1984, he was appointed as an Assistant Professor with The University of Michigan, Ann Arbor, MI, USA, and become a Full Professor, in 1994. He has also served as the Director of the Radiation Laboratory, from 1998 to 2000. From 2003 to 2017, he was a Roy and Lois Chope Chair Professor of engineering with The Ohio State University, and served as the Director of the ElectroScience Laboratory, from 2003 to 2016. Since 2017, he has been the Dean of the College of Engineering and Computing and a Professor of electrical and computer engineering with Florida International University.

Over the years, he carried out research in antennas, wireless communications and propagation, computational methods, electromagnetic compatibility and interference, design optimization, RF materials, multiphysics engineering, millimeter waves, terahertz and medical sensing. His publications include eight books, 420 journal papers, nearly 800 conference papers, and 26 book chapters, and holds 17 patents/patent disclosures. Among his co-authored books are *Approximate Boundary Conditions in Electromagnetics* (1995), *Finite Element Methods for Electromagnetics* (1998), *Antenna Engineering Handbook* (2007, fourth edition), *Small Antennas* (2010), and *Integral Equation Methods for Electromagnetics* (2011). He has graduated/mentored 90 doctoral students/post-docs with 41 of them receiving best paper awards at conferences. His service to Professional Societies include: the 2004 President for the IEEE Antennas and Propagation Society (2004), the Chair for USNC/URSI Commission B (2015–2017), twice a General Chair for the IEEE Antennas and Propagation Symposium, the IEEE APS Distinguished Lecturer, the IEEE APS Fellows Committee Chair, the IEEE-Wide Fellows Committee Member, and an associate editor for several journals. He was listed by ISI among the top 250 most referenced authors (2004), and he is a Fellow of ACES. Among his awards are: The University of Michigan College of Engineering Research Excellence Award (1993), the Scott Award from The Ohio State University College of Engineering for Outstanding Academic Achievement (2011), the IEEE AP Society C-T. Tai Teaching Excellence Award (2011), the IEEE Henning Mentoring Award (2013), the IEEE Antennas & Propagation Distinguished Achievement Award (2014), The Ohio State University Distinguished Scholar Award (2016), and The Ohio State University ElectroScience George Sinclair Award (2017). He is a Fellow of the Applied Computational Electromagnetics Society.